SAND2000-0318J

# The Impact of Process Parameters on Gold Elimination from Soldered Connector Assemblies[1]

P.T. Vianco
A. C. Kilgo

Sandia National Laboratories
Albuquerque, NM USA

RECEIVED
FEB 24 2000
OSTI

## Abstract

Minimizing the likelihood of solder joint embrittlement in connectors is realized by reducing or eliminating retained Au plating and/or Au-Sn intermetallic compound formation from the assemblies. Gold removal is performed most effectively by using a double wicking process. When only a single wicking procedure can be used, a higher soldering temperature improves the process of Au removal from the connector surfaces and to a nominal extent, removal of Au-contaminated solder from the joint. A longer soldering time did not appear to offer any appreciable improvement toward removing the Au-contaminated solder from the joint. Because the wicking procedure was a manual process, it was operator dependent.

*Key words: connectors, soldering, gold embrittlement*

## Introduction

Several field failures of cable assemblies similar to that shown by photograph in Fig. 1a were reported. The solder interconnects were suspected. The cut-away macrograph in Fig. 1b and schematic diagram in Fig. 1c show that the assembly has two solder joints. The first solder joint is that formed between the center pin of the connector and the center conductor of the cable. The center conductor of the cable is a Cu-plated steel wire (male) having a Ag plating over the Cu. The Ag layer is not necessarily sacrificial because it is not fully consumed in the soldering process. The connector center pin, which has the cup (female) geometry, is made of steel that is coated with a Ni/Au electroplated finish. The Ni coating forms the solderable finish while the Au coating is the protective (sacrificial) finish that maintains the solderability of the underlying Ni layer prior to, and during, soldering.

The Au coating is removed from the center pin cup by a hot solder "wicking" process. The cup is first filled with molten 63Sn-37Pb (wt.%) solder. Then, the solder is removed or wicked out of the hole. The objective of this procedure is to have the Au coating dissolve into the molten solder and then be removed from the cup with the withdrawal of the solder,

[1] Sandia is a multiprogram laboratory operated by Sandia Corp., a Lockheed Martin Company, for the United States Dept. Of Energy under contract DE-AC04-94AL85000.

## DISCLAIMER

This report was prepared as an account of work sponsored by an agency of the United States Government. Neither the United States Government nor any agency thereof, nor any of their employees, make any warranty, express or implied, or assumes any legal liability or responsibility for the accuracy, completeness, or usefulness of any information, apparatus, product, or process disclosed, or represents that its use would not infringe privately owned rights. Reference herein to any specific commercial product, process, or service by trade name, trademark, manufacturer, or otherwise does not necessarily constitute or imply its endorsement, recommendation, or favoring by the United States Government or any agency thereof. The views and opinions of authors expressed herein do not necessarily state or reflect those of the United States Government or any agency thereof.

## DISCLAIMER

Portions of this document may be illegible in electronic image products. Images are produced from the best available original document.

leaving only a Sn-Pb solder coating on the inside surface. This procedure is performed in order to prevent Au embrittlement of the final solder joint that is made between the cable conductor and the center pin. This solder joint is the subject of the investigation, the results of which are reported upon in this paper.

For the record, the second solder joint is that formed between the connector housing and the cable outer sleeve. The connector housing is steel with a Ni/Au coating which serves the same purposes as it is does on the center pin. A hot solder dipping process is used to replace the Au layer with a Sn-Pb finish. The cable sleeve is made of Cu and is soldered to the connector in this form.

Earlier studies exposed cable assemblies to accelerated life aging environments (Vianco, 1997; Vianco, 1998). Those environments included thermal cycling, thermal shock, as well as mechanical shock and vibration conditions., The subsequent metallographic cross sections of the cable solder joints revealed that cracks were present in the center pin/cable center conductor solder joints in 63% of the sample lot. The cracks were not of sufficient extent to cause electrical malfunction. The source of the cracks appeared to be Au embrittlement of the solder, suggesting that the specified wicking process had been ineffective at removing the initial Au coating from the inner cup surface of the pin.

In response to that finding, as second study was performed on similar assemblies which had not been exposed to accelerated testing environments. Seven such assemblies were cross sectioned to reveal the center pin/cable conductor solder joint. A total of 29% of those solder joints exhibited cracking. Again, the suspected cause was Au embrittlement of the Sn-Pb solder. This latter result confirmed that cracking of the solder joints had likely occurred at the time of, or shortly after, assembly.

It was deemed critical that the effectiveness of the wicking process be more fully characterized and the procedure then be corrected with this added information. The evaluation was carried out on the joint formed by soldering the connector and cable together *after* the wicking process had been performed. The investigation reported here examined the effect of four wicking parameters on the solder joint metallurgy. The four parameters were: (1) soldering temperature, (2) soldering hold time, (3) the number of wicking steps or "immersions" with Sn-Pb solder practiced on the center pin cup prior to the cable assembly, and (4) the particular operator performing the task. The details of these procedures and the follow-up analysis are presented in the following section.

## Experimental procedures

*Process matrix.*

Two certified soldering operators were selected for the assembly process; they were simply designated #1 and #2. Two soldering process temperatures were used:

Parameter "3.7" ... low temperature

Parameter "4.1" ... high temperature

The parameters, 3.7 and 4.1, were actually the settings as designated on the soldering iron control panel. Two elapsed times during which the molten solder remains in contact with the cup were evaluated; those periods are:

Parameter "4" ... 4 seconds

Parameter "8" ... 8 seconds

The number of solder filling/wicking procedures conducted was either *once* or *twice* prior to the soldering of the cable lead to the cup. Therefore, based upon the variables of: soldering temperature, soldering time, number of immersions, and number of operators, there were 16 possible combinations. Triplicate assemblies were made per each experimental matrix condition.

*Evaluation metrics.*

Shown in Fig. 2 is a schematic representation of a cross section taken through the connector center pin/cable center conductor solder joint on which the defect analysis was performed. The solder joints were evaluated at, and a quantitative metric assigned to, the mouth location ("M" ), the center location ("C"), and the end location ("E") of the joint. Both "sides" of the joint were evaluated, albeit the two views are of the same joint. The metric values from both sides of the joint were combined. These data were then joined with similar results from the other two cases from amongst the triplicate samples. The assignment of the quantitative metrics is described below.

First, a survey was made for cracks in the solder joints. A discrete metric was used to describe cracking: 0 when no cracking was observed, or 1 in the case when cracking was observed at the location.

A variable metric was used to describe the following properties: (1) the presence of Au-Sn intermetallic compound, either as a layer on the connector housing surface or as needles within the solder microstructure; (2) the presence of Au plating on the cup surface, (3) the thickness of the Ag plating that remained on the cable center conductor surface; and (4) the thickness of the Ni plating layer on the connector (center contact) cup. The Au-Sn intermetallic compound layer and/or needle formation (1), as well as the extent of retained Au finish (2), provided a measure of the effectiveness of the wicking process to remove Au from center pin cup. The Au layer metric indicates the extent to which Au has been removed

from the connector cup surface. The retention of Au on the cup surface raises the likelihood of further intermetallic compound layer formation in service by means of solid-state diffusional processes and thusly, an increased chance of solder joint embrittlement and cracking.

The Au-Sn intermetallic compound metric describes the extent to which the Au is present in the solder. In the event that the Au was fully dissolved from the connector surface, yet remained in the solder, then the joint is still be highly susceptible to embrittlement when Au-Sn needles form after solidification of the contaminated solder. Therefore, these two metrics, retained Au plating and Au-Sn intermetallic compound formation, provided the crucial indicators of the potential for solder joint embrittlement and crack formation.

The Ag-coating metric (3) is a measure of the thickness of Ag plating that is retained on the cable center conductor after completion of the connector-to-cable soldering operation. The cable is soldered into the connector cup after the solder wicking procedures had been performed on the latter structure. Therefore, intuitively, there should be no significant, first-order dependence shown by the Ag layer thickness on the connector solder wicking activity. Only the final connector-to-cable assembly operations should affect the Ag thickness. Nevertheless, this parameter was assessed in order to make certain that no second-order effects from the wicking procedures impacted the Ag thickness. These added analyses were performed because, in the event that an unanticipated, secondary effect by the solder wicking operations did cause an inadvertent loss of Ag plating thickness, there would be potential consequences to the final soldering step that attaches the connector cup to the cable conductor. Because it cannot be assumed that the underlying Cu wire surface is solderable, a significant or complete loss of the Ag plating could potentially result in a deterioration of the cable conductor solderability and hence, an increased occurrence of solder joint defects in the connector/cable assembly.

Also, an evaluation was made of the Ni solderable layer thickness which lies under the Au plating layer. Loss of the Ni layer would result in a deterioration of solderability, since the underlying connector structure is, in fact, not solderable. The consequence would be an increase in solder joint defects. It was observed that in all cases, a negligible quantity of Ni layer was lost to the molten solder. Therefore, this metric was not listed in further analyses.

The quantitative metrics for each of these features are described as follows:

| | | |
|---|---|---|
| (1) Au-Sn intermetallic compound needles/layer | ..... | 0 (none) - 5 (numerous) |
| (2) Au-plating remaining | ..... | 0 (none) - 5 (full, unsoldered) |

on connector center cup

(3) Ag-coating thickness ..... 0 (none) - 5 (full, unsoldered)
on cable center conductor

(4) Ni-coating thickness ..... 0 (none) - 5 (full, unsoldered)
on connector center cup

As noted above, the values of each metric were determined on both sides of the joint; those values were combined with the similar measurements from all of the triplicate samples. A mean was determined from the six values compiled per metric, per location of the solder joint, and per assembly process (time, temperature, and operator). A scatter term was represented by $\pm$ one standard deviation of the data.

It is important to note that the above evaluations were performed without knowledge of the assembly parameters or operator. A sample number was used to reference the particular solder joint. It was only during the data compilation that each sample (number) became associated with a particular set of process parameters (time and temperature) as well as operator. Finally, the plating thickness on each connector was provided by the assembler prior to the soldering operations.

**Results**

The defect metrics data are compiled per operator in Table 1. However, it is more instructive to compare the results graphically. Scatter values ($\pm$ one standard deviation) have been left out of plots for clarity; the reader is referred to Table 1 for those parameters.

*Retained Au plating.*

Shown in Fig. 3a is a graph of the metric describing the extent of original Au plating that has been retained on the center connector cup wall at the mouth location, "M," of the solder joint (0, none to 5, complete). The x-axis includes the independent variables of operator (#1 and #2) and wicking frequency (1, 2). The single wicking operation data indicates an increased propensity for the Au plating layer to be present in joints formed by operator #2 versus operator #1. The extent of retained Au after one wicking step was reduced for either operator by increasing the soldering temperature. This latter observation is more clearly shown in Fig. 3b which is a plot of the retained Au plating as a function of soldering temperature. The data were grouped per number of wicking operations. The temperature dependence of retained Au plating is commensurate with the fact that the rate of Au dissolution into molten solder increases with higher temperatures.

It is noted from the plots in Figs. 3a and 3b that primarily, with one wicking process and the lower soldering temperature (3.7), more Au was retained after the *longer* soldering time (8s) than was the case for the shorter soldering time period (4s). This trend was observed, irrespective of the operator. Intuition would suggest that longer soldering times should provide a better opportunity for the Au to be dissolved away from the substrate and into the solder. As is discussed in detail below, the observed trends in the retained Au layer were not attributable to differences in the nominal Au thickness on the connector structures. Of course, localized variations in the Au plating thickness, particularly at the joint mouth where the throwing power of the bath would be greater, were not assessed and, therefore, cannot be ruled out. The only phenomenon that would explain these observations was that any Au already dissolved in the solder had, in fact, precipitated back on to the substrate wall during the longer hold time. The author is aware of only one such recorded observation of such a mechanism (Mei, 1998). In that cited work, solid-state diffusion was surmised to be the mechanism responsible for dissolved Au to migrate back to the solder (Sn-Pb)/substrate (Ni layer) interface. It is not known whether a similar mechanism is active when the solder is in the liquid state.

The results in Fig. 3 do show that increasing the number of wicking operations from one to two had a significant impact on the retained Au layer metric. On the right-hand side of Fig. 3a, the data indicated that the presence of retained Au at the joint mouth was reduced to nearly zero for both operators following the second immersion step. Also, any differences in the retained Au thickness caused by the temperature or time variables, were all but eliminated by using the double wicking process.

Similar analyses of retained Au plating were not required at the center (C) and end (E) locations in the joint because Au was completely absent there in *all* cases (Table 1).

*Au-Sn needle formation.*

Next, the evaluation turned to the presence of Au-Sn needles in the solder joints. A plot of the metric describing the presence of Au-Sn needles (0, none to 5, numerous) at the mouth (M) of the joint as a function of the operator and number of wicking operations is shown in Fig. 4a. The left-hand side of the x-axis compares the performance of operators #1 and #2 with the use of a single wicking process; the right-hand side compares the two operators with two wicking operations. Each curve represents different soldering time-soldering temperature combinations. For a single wicking step and irrespective of temperature and time conditions, fewer needles were reported with operator #1 than with operator #2. However, the addition of a second wicking step caused the propensity for Au-Sn needles to drop to nearly zero for all test conditions and operators.

The plot in Fig. 4a also showed that a higher soldering temperature benefited both operators toward eliminating the Au-Sn needles from the mouth location in the joint when only one wicking operation was in use. This point is more clearly illustrated in Fig. 4b. Fig. 4b is a composite plot of the Au-Sn needle metric as a function of soldering temperature, combining the effects of a single wicking process (left-hand side) with the double wicking process (right-hand side). That plot shows that an increased temperature was of greatest benefit to operator #2 for whom the Au-Sn needles were most numerous.

The dependence of Au-Sn needle presence as a function on soldering time was most pronounced with the single wicking step as is illustrated by the left-hand side of Fig. 4b. It was noted that more Au-Sn needles were observed after the *longer* immersion times per each soldering temperature and operator. This observation would suggest, initially, that the longer wicking times allowed more of the Au to be dissolved from the connector wall into the molten solder. However, this explanation would contradict the retained Au layer data in Figs. 3a and 3b. An explanation of these seemingly contradictory behaviors has as yet not been determined.

When a second immersion process was added, the presence of Au-Sn needles as well as differences between operators, temperature, and time conditions were all but eliminated. A simple, generalized mechanism begins with the first immersion which removes Au from the connector cup wall. The dissolved Au resided in the solder, either in solution or as precipitated Au-Sn needles. The second wicking process then removed the contaminated solder (along with any remaining Au plating as implied by Fig. 3) which contained the dissolved Au and Au-Sn needles (Fig. 4), leaving behind a "clean" coating for the final joint between the connector cup and the cable conductor.

The Au-Sn needles were also observed at locations further into the joint structure, at the center (C) and end (E) positions. Shown in Fig. 5a is a plot of the Au-Sn needle metric as a function of soldering temperature and wicking frequency at the center (C) position of the joint. A similar plot representing needle prevalence at the end location in the joint is shown in Fig. 5b. The data in Fig. 5a show that Au-Sn needles were only observed at the lower soldering temperature, when a single wicking step was used, and only in joints made by operator #2. The dependence of the metric on soldering time reproduced the results in Fig. 4; a longer soldering time resulted in a greater concentration of Au-Sn needles. Increasing the soldering temperature eliminated the needles entirely from the joint as did using a double wicking process. Needle formation was not observed in the work of operator #1 under all circumstances.

The plot in Fig. 5b indicated that Au-Sn needles were observed at the end (E) position of the joint under the following combination of parameters: 3.7 temperature, 8 s

soldering time, and operator #2. The already nominally low metric value was brought to zero by increasing the soldering temperature or using a double wicking procedure.

*Summary of the retained Au plating and Au-Sn needle metrics*

The data presented in Figs. 3, 4 and 5 can be compiled into the following synopsis. (1) Reducing the likelihood of solder joint Au embrittlement by reducing or eliminating retained Au plating and/or minimizing Au-Sn needle formation, was realized most effectively by using a double wicking process. That is because two wicking steps provide for *both* an increased efficiency for Au removal from the connector surfaces *as well as* optimum removal of the Au-contaminated solder from the joint prior to final assembly. The data showed that the double wicking procedure removed any significant dependencies exhibited by these either metric on soldering temperature, soldering time, or operator. (2) In the event that the double wicking process proves to be an unacceptable alternative to the single step procedure, then the next best step is to use the operator #1 in this procedure. For each of the four possible combinations of soldering time and soldering temperature, operator #1 gave better results than operator #2 in three of those four circumstances. This trend clearly points to a significant impact had by operator skill with the current procedure. (3) Again, when only a single wicking procedure can be used, a higher soldering temperature improves the process of Au removal from the connector surfaces and, to some extent, enhances removal of Au-contaminated solder from joint by either operator. (4) Lastly, a longer soldering time did not always assure that the Au plating was completely dissolved from the connector shell wall, although the greater amount of Au-Sn needles in the solder would suggest to the contrary.

*Effect of Au plating thickness on retained Au layer thickness and the propensity for Au-Sn needle formation.*

The starting thickness of the Au plating layer could potentially impact the amount of Au retained on the surfaces as well as the propensity for Au-Sn needle formation in the joints. Shown in Fig. 6a is a plot of the retained Au layer metric at the "M" location for operator #1 as a function of the recorded Au thickness. No correlation was observed between the two parameters. A similar assessment was made for the solder joints made by operator #2 (Fig. 6b). The presence of Au-Sn needles also did not correlate with the starting thickness of the Au deposit. This point is exemplified by the plots in Figs. 6c, 6d, and 6e for solder joints made by operator #2. Similar results were recorded for operator #1. In summary, the metrics of retained Au and Au-Sn needle formation did not correlate with the Au plating thickness values for the connectors.

*Ag-plating thickness.*

The third metric for evaluation was that of the thickness of the Ag plating that remained on the cable center conductor. Shown in Fig. 7a is a plot of the extent of the Ag plated layer that was retained after the soldering processes at the mouth location "M" of the joint as a function of the soldering temperature (low, 3.7 and high, 4.1) and the number of wicking steps (1 or 2). Each curve represented the combination of operator (#1 or #2) and soldering time (4 s or 8 s). It is observed that the Ag thickness was not significantly reduced under any of the soldering conditions. Analyses of the plating thickness were performed for the center location, "C," and the end location, "E;" those data are shown in Figs. 7b and 7c, respectively. In both of the latter cases, decreases in the layer thickness were observed which became increasingly greater from the "M" location, to the "C" location, and finally at the "E" location. The Ag plating layer thickness decreases that were observed at either "C" or "E" locations exhibited no significant dependencies on any of the wicking parameters used to solder coat the connector cup. These observations confirmed that the range of wicking procedure parameters used in this study did not, as variables, have a significant, nominal impact on the Ag-plating thickness that remained on the cable center conductor after the final assembly process. Lastly, it was also observed that the thickness of the Ag-plating layer remained adequate to minimize solderability-related defects, even at its thinnest value near the end ("E") of the joint.

**Conclusions**

[1] Minimizing the likelihood of solder joint Au embrittlement in connector assemblies that use Au/Ni plated piece parts was realized most effectively by using a double wicking process. The data showed that the double wicking procedure removed any significant dependencies exhibited by the retained Au layer and/or Au-Sn intermetallic compound metrics on soldering temperature, soldering time, or operator.

[2] As a manual procedure, the solder wicking step was sensitive to the particular operator performing it. Operator #1 produced better results than operator #2 in three of the four possible combinations of soldering time and soldering temperature.

[3] When only a single wicking procedure can be used, a higher soldering temperature improved the process of Au removal from the connector surfaces and to a more limited extent, the elimination of Au-Sn intermetallic compound contaminated solder from joint.

[4] A longer soldering time did not appear to offer any appreciable improvement toward removing the Au-contaminated solder from the joint and in some cases, degraded the conditions.

[5] The thickness of the Ag-plating on the cable center conductor after the assembly process decreased from the mouth ("M") of the joint towards the end ("E") position. However, the thickness parameter, at any location, was independent of the parameters used to perform the initial wicking operation.

[6] No correlation was observed between the retained Au layer thickness or the Au-Sn needle formation metrics and the initial Au plating thickness, irrespective of the particular operator.

**Acknowledgments:**

The authors wish to thank G. Becka and G. Brown of Honeywell AF&T who supervised the cable assembly routine and provided the mounted specimens as well as J. Hanlon at Sandia National Laboratories for his helpful comments in the course of this study.

**References:**

[1] Vianco, P. "MC4395 Connector Solder Joint Analysis," *memorandum to J. Hanlon*, dtd. December 22, 1997, Sandia National Laboratories, Albuquerque, NM.

[2] Vianco, P."MC4395 Connector Solder Joint Analysis - Part II," *memorandum to J. Hanlon*, dtd. January 12, 1998, Sandia National Laboratories, Albuquerque, NM.

[3] Mei, Z, et al. 1998, "Brittle Interfacial Fracture of PBGA Packages Soldered on Electroless Nickel/Immersion Gold," *Proc. 48$^{th}$ ECTC*, p. 952.

**Table 1**
**Compiled Metrics Data of Defects in the Solder Joints Formed Between the Connector (MC4395Center Pin and Cable Center Conductor**
Position in the joint - M: mouth; C: center; E: end
() ± one standard
*Mount numbers corresponding to time, temp., and wicking parameters.*

| Time | Temp. | No. of | Au-Sn Needles | | | Ag Plate | | | Au Plate | | |
|---|---|---|---|---|---|---|---|---|---|---|---|
| 4,8 s | 3.7,4.1 | Wicks | M | C | E | M | C | E | M | C | E |
| **Operator #1** | | | | | | | | | | | |
| 4 | 3.7 | 1 | 0.83 | 0 | 0 | 5.00 | 3.67 | 1.50 | 0.17 | 0 | 0 |
| *(22, 44, 45)* | | | (1.60) | | | (0.00) | (1.03) | (1.72) | (0.40) | | |
| 4 | 3.7 | 2 | 0 | 0 | 0 | 5.00 | 3.00 | 1.00 | 0 | 0 | 0 |
| *(1, 13, 17)* | | | | | | | (0.00) | (0.63) | (1.10) | | |
| 4 | 4.1 | 1 | 0.67 | 0 | 0 | 5.00 | 4.00 | 2.33 | 0 | 0 | 0 |
| *(3, 11, 29)* | | | (1.03) | | | (0.00) | (0.89) | (1.21) | | | |
| 4 | 4.1 | 2 | 0 | 0 | 0 | 5.00 | 2.83 | 0.50 | 0 | 0 | 0 |
| *(6, 36, 37)* | | | | | | (0.00) | (0.41) | (0.55) | | | |
| 8 | 3.7 | 1 | 2.17 | 0 | 0 | 5.00 | 2.67 | 0.67 | 0.83 | 0 | 0 |
| *(19, 30, 41)* | | | (1.33) | | | (0.00) | (0.82) | (1.21) | (2.04) | | |
| 8 | 3.7 | 2 | 0 | 0 | 0 | 5.00 | 3.00 | 0.50 | 0 | 0 | 0 |
| *(7, 16, 46)* | | | | | | (0.00) | (1.67) | (0.55) | | | |
| 8 | 4.1 | 1 | 0.83 | 0 | 0 | 5.00 | 3.83 | 0.83 | 0 | 0 | 0 |
| *(8, 24, 31)* | | | (1.33) | | | (0.00) | (0.89) | (1.17) | | | |
| 8 | 4.1 | 2 | 0.66 | 0 | 0 | 5.00 | 3.17 | 1.50 | 0 | 0 | 0 |
| *(12, 27, 35)* | | | (1.03) | | | (0.00) | (0.75) | (1.38) | | | |

*con't*

**Table 1 (con't)**
**Compiled Metrics Data of Defects in the Solder Joints Formed Between the Connector (MC4395Center Pin and Cable Center Conductor**
Position in the joint - M: mouth; C: center; E: end
() ± one standard
*Mount numbers corresponding to time, temp., and wicking parameters.*

| | | | | | | | | | | | |
|---|---|---|---|---|---|---|---|---|---|---|---|
| **Operator #2** | | | | | | | | | | | |
| 4 | 3.7 | 1 | 3.50 | 1.00 | 0 | 5.00 | 3.17 | 1.50 | 1.00 | 0 | 0 |
| *(10, 32, 34)* | | | (1.52) | (1.55) | | (0.00) | (1.17) | (1.64) | (1.55) | | |
| 4 | 3.7 | 2 | 0.33 | 0 | 0 | 5.00 | 3.67 | 1.00 | 0.83 | 0 | 0 |
| *(9, 28, 40)* | | | (0.82) | | | (0.00) | (1.03) | (1.09) | (2.04) | | |
| 4 | 4.1 | 1 | 1.50 | 0 | 0 | 5.00 | 4.00 | 1.00 | 0.83 | 0 | 0 |
| *(5, 14, 18)* | | | (1.76) | | | (0.00) | (0.89) | (1.10) | (2.04) | | |
| 4 | 4.1 | 2 | 0.16 | 0 | 0 | 5.00 | 4.00 | 1.83 | 0 | 0 | 0 |
| *(21, 39, 48)* | | | (0.41) | | | (0.00) | (0.89) | (1.17) | | | |
| 8 | 3.7 | 1 | 4.83 | 2.50 | 1.00 | 5.00 | 3.00 | 1.67 | 3.67 | 0 | 0 |
| *(2, 38, 42)* | | | (0.41) | (1.65) | (1.67) | (0.00) | (0.00) | (0.52) | (2.16) | | |
| 8 | 3.7 | 2 | 0 | 0 | 0 | 5.00 | 3.83 | 2.17 | 0.33 | 0 | 0 |
| *(23, 33, 43)* | | | | | | (0.00) | (0.75) | (1.47) | (0.52) | | |
| 8 | 4.1 | 1 | 2.50 | 0 | 0 | 5.00 | 2.83 | 1.00 | 0.33 | 0 | 0 |
| *(15, 26, 47)* | | | (2.74) | | | (0.00) | (0.75) | (1.26) | (0.52) | | |
| 8 | 4.1 | 2 | 0 | 0 | 0 | 5.00 | 3.33 | 1.00 | 0 | 0 | 0 |
| *(4, 20, 25)* | | | 0 | | | (0.00) | (1.37) | (1.10) | | | |

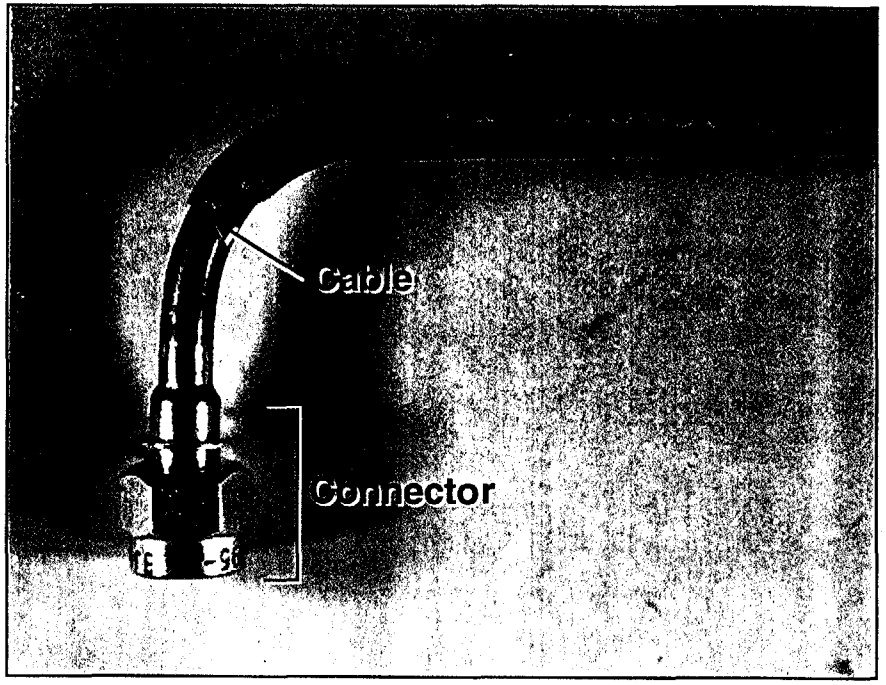


**(a)**

Fig. 1 (a) Photograph, (b) cross section macrograph, and (c) schematic diagram (not to scale) of the connector center pin/cable center conductor solder joint and the connector housing/cable outer sleeve solder joint.

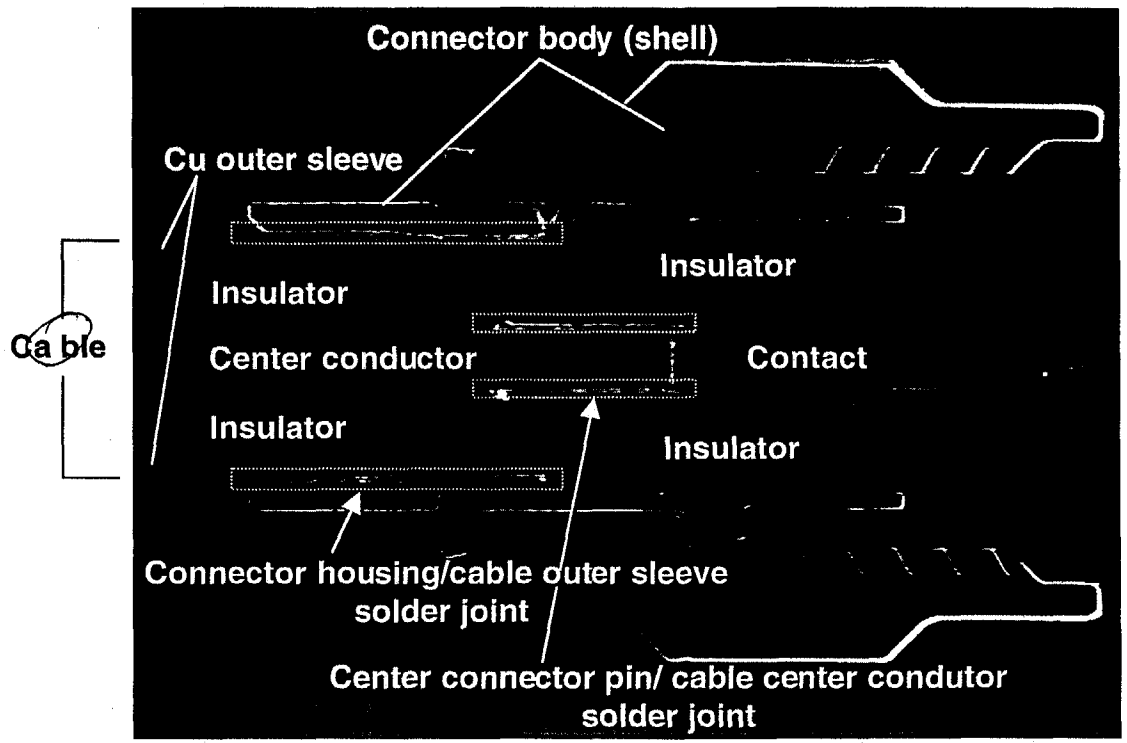
Connector body (shell)
Cu outer sleeve
Insulator
Insulator
Cable
Center conductor
Contact
Insulator
Insulator
Connector housing/cable outer sleeve solder joint
Center connector pin/ cable center condutor solder joint

Fig. 1(b)

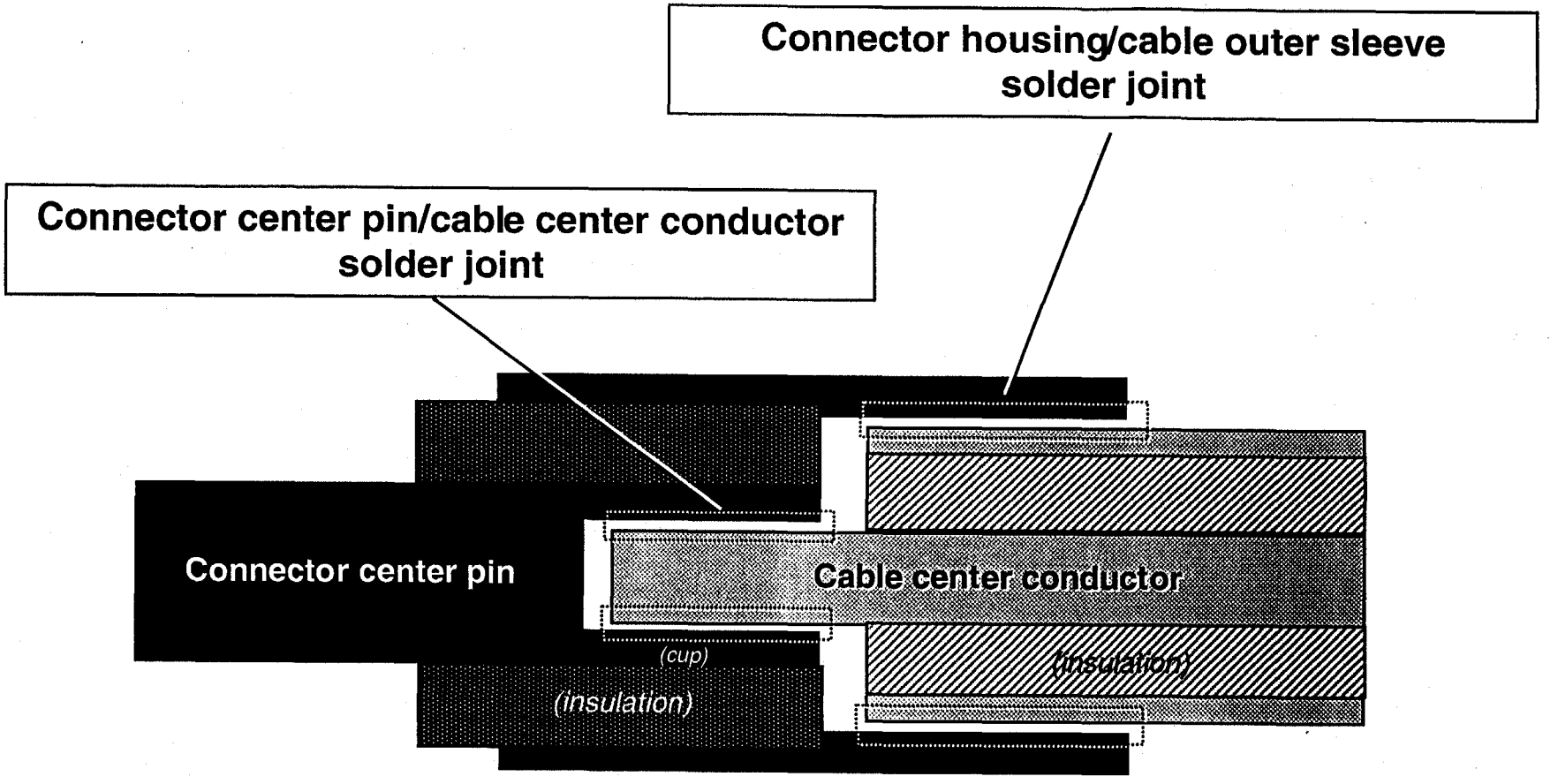
Connector housing/cable outer sleeve solder joint
Connector center pin/cable center conductor solder joint
Connector center pin
Cable center conductor
(cup)
(insulation)
(insulation)

Fig. 1(c)

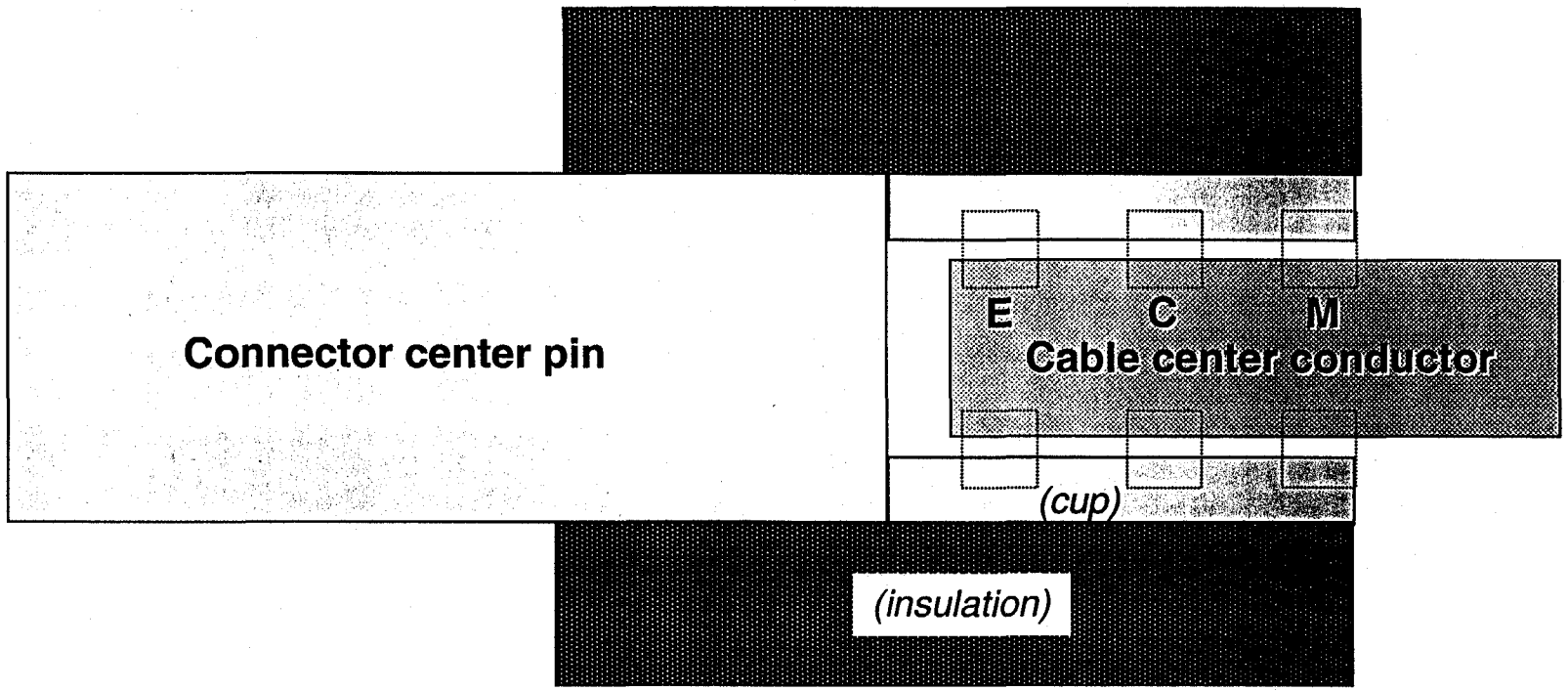


Fig. 2 Schematic diagram of the connector center pin/cable center conductor solder joint showing the locations at which the assessment for cracks, Au plating, and Au-Sn intermetallic compound formation were made: "M," mouth; "C," center; and "E," end.

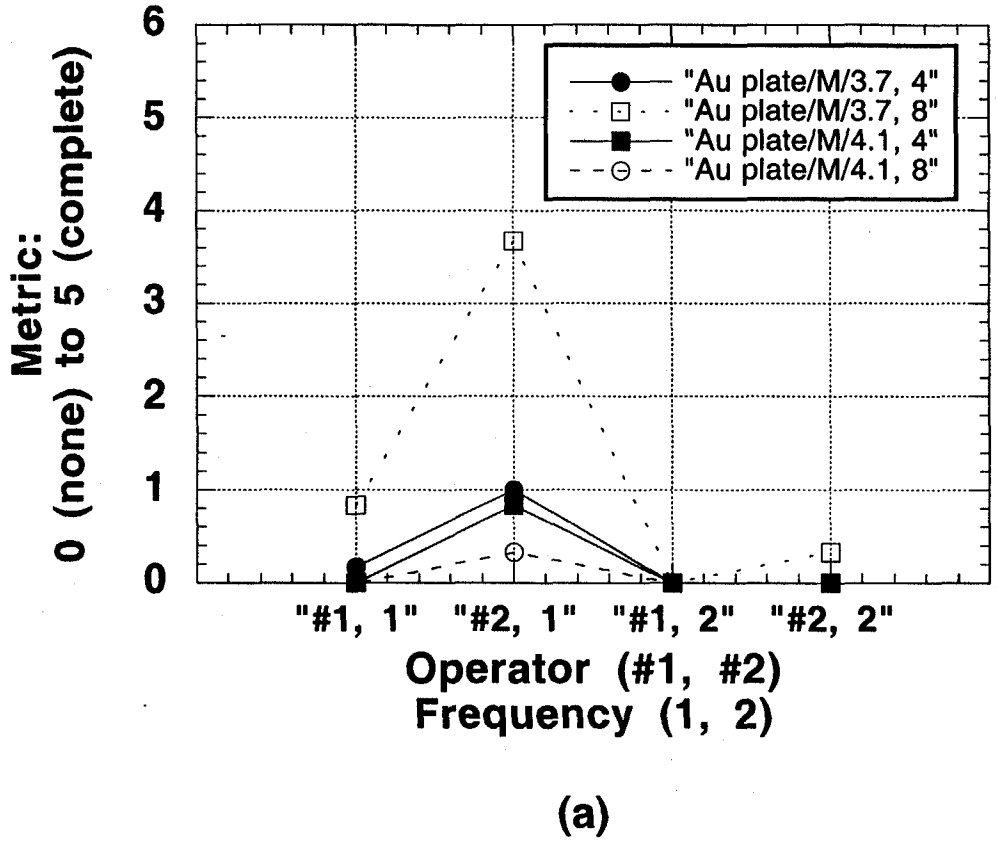


(a)

Fig. 3 (a) Graph of the metric representing the retained Au plating (0, none versus 5, complete thickness) as a function of operator (#1 or #2) and the number of wicking operations (1 or 2) at the mouth, "M," location of the joint. Different curves pertain to the combinations of soldering temperature (low, 3.7 and high, 4.1) and soldering time (4 and 8 s). (b) The retained Au plating metric as a function of soldering temperature (low, 3.7 and high, 4.1)and the number of wicking steps (1 or 2) at the "M" location. The different curves represent the combinations of operator (#1 or #2) and soldering time (4 s or 8 s).

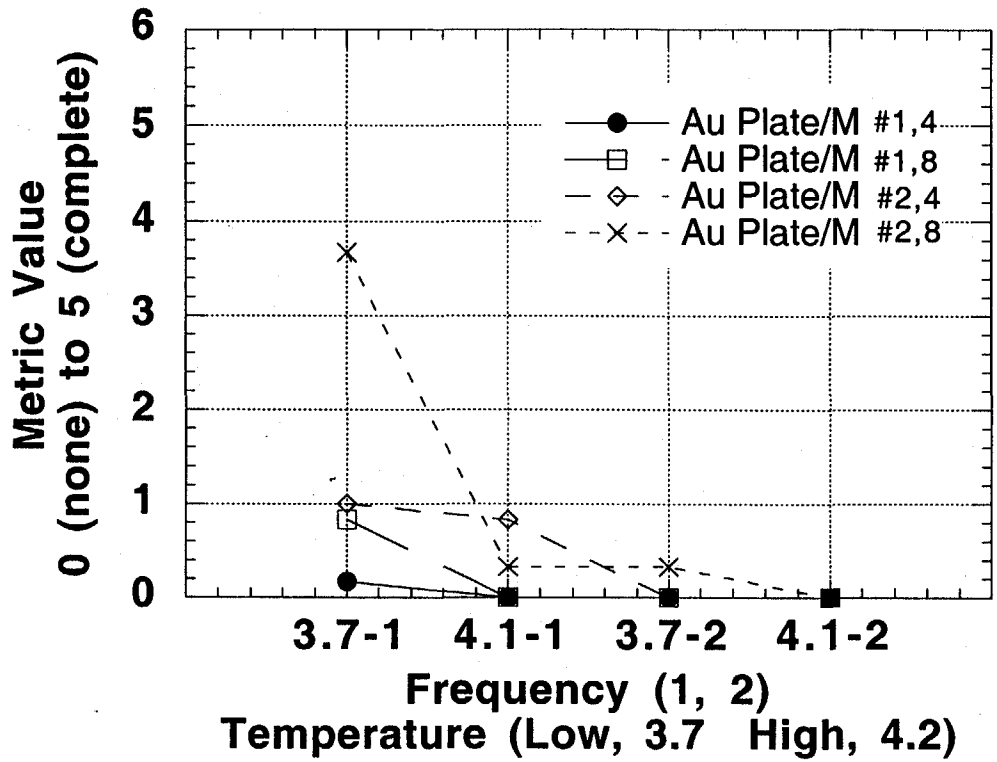
Metric Value
0 (none) to 5 (complete)
6
5
4
3
2
1
0
Au Plate/M #1,4
Au Plate/M #1,8
Au Plate/M #2,4
Au Plate/M #2,8
3.7-1
4.1-1
3.7-2
4.1-2
Frequency (1, 2)
Temperature (Low, 3.7 High, 4.2)

Fig. 3(b)

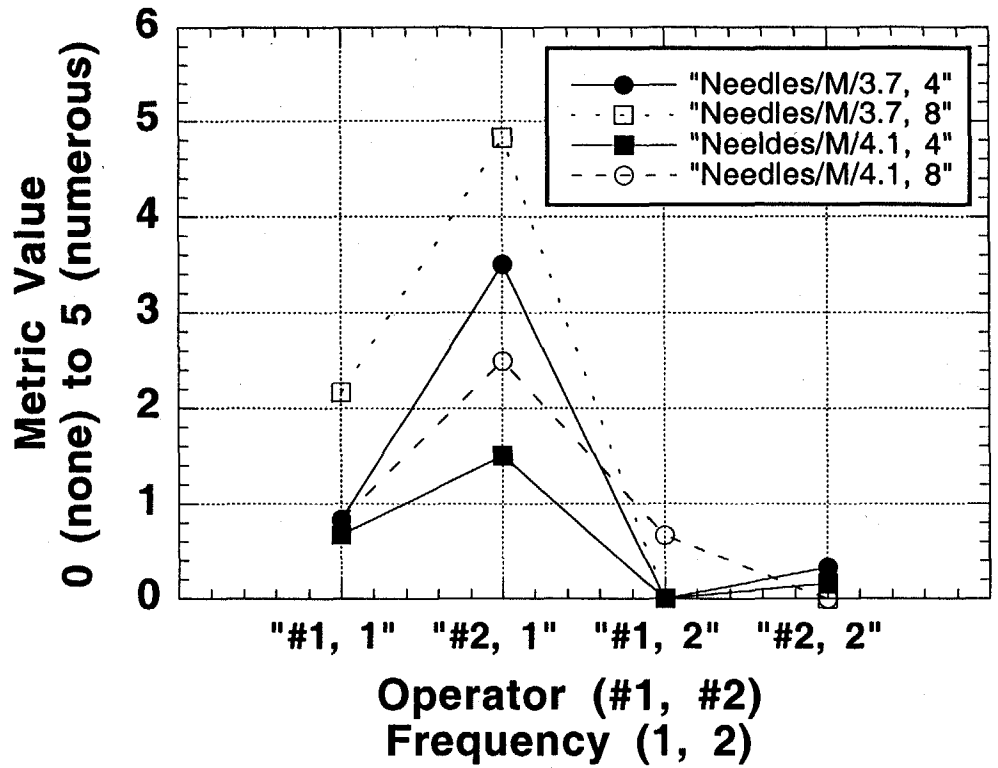


(a)

Fig. 4 (a) Graph of the metric representing Au-Sn needles (0, none versus 5, numerous) as a function of operator (#1 or #2) and the number of wicking operations (1 or 2) for the mouth location, "M," of the joint. Different curves pertain to the combinations of soldering temperature (low, 3.7 and high, 4.1) and soldering time (4 and 8 s). (b) Gold-tin needle metric as a function of soldering temperature (low, 3.7 or high, 4.1) and the number of wicking steps (1 or 2) at the "M" location. The different curves represent the combinations of operator (#1 or #2) and soldering time (4 s or 8 s).

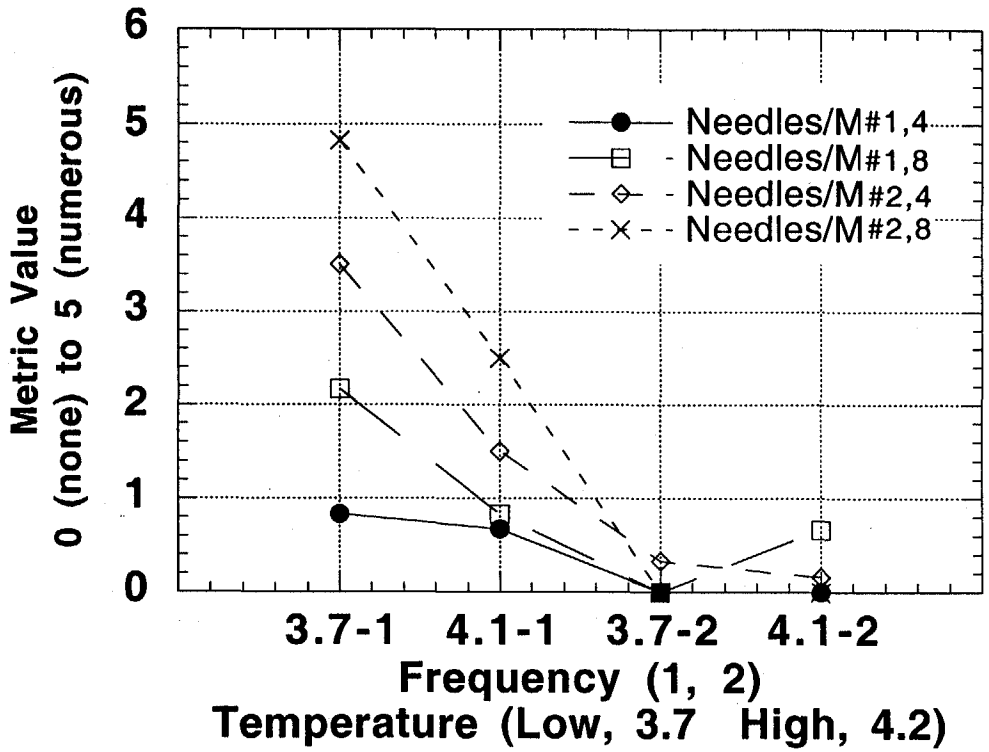
Metric Value
0 (none) to 5 (numerous)
6
5
4
3
2
1
0
Needles/M#1,4
Needles/M#1,8
Needles/M#2,4
Needles/M#2,8
3.7-1
4.1-1
3.7-2
4.1-2
Frequency (1, 2)
Temperature (Low, 3.7 High, 4.2)

Fig. 4(b)

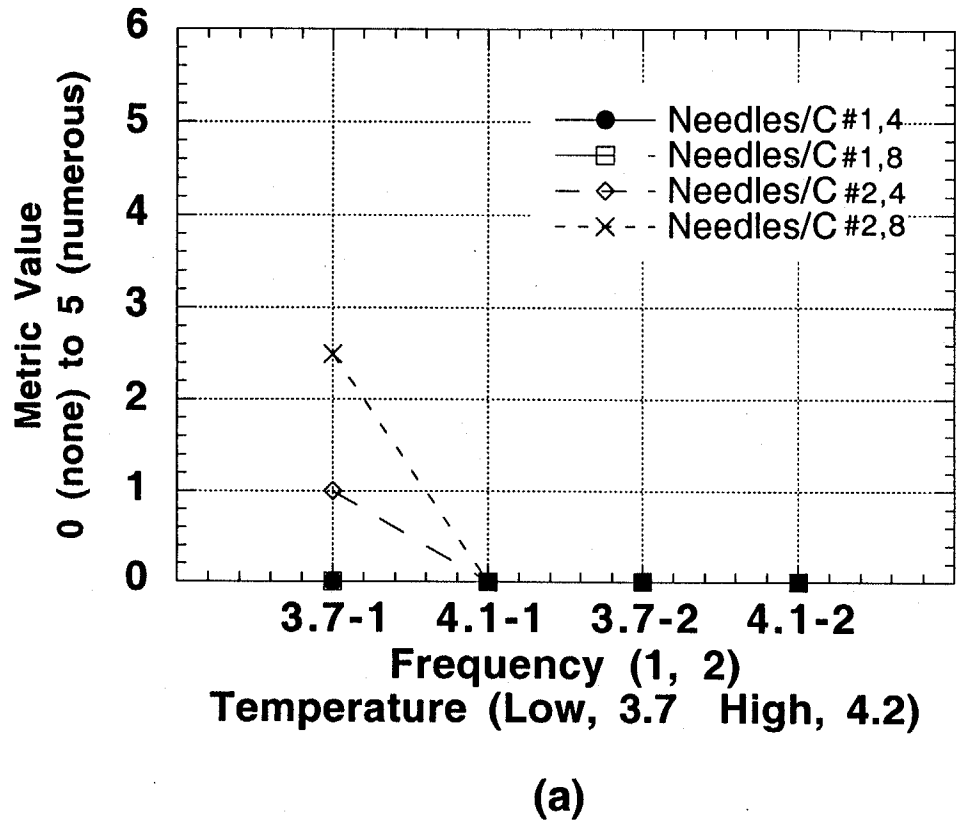


(a)

Fig. 5 (a) Graph of the Au-Sn needles metric as a function of the soldering temperature (low, 3.7 and high, 4.1)and the number of wicking steps (1 or 2) at the center location, "C," of the joint. Each curve represents the combinations of operator (#1 or #2) and soldering time (4 s or 8 s). (b) Graph of the Au-Sn needles metric as a function of the soldering temperature (low, 3.7 and high, 4.1) and wicking frequency (1 or 2) at the end location, "E," of the joint. Each curve represents the combination of operator (#1 or #2) and soldering time (4 s or 8 s).

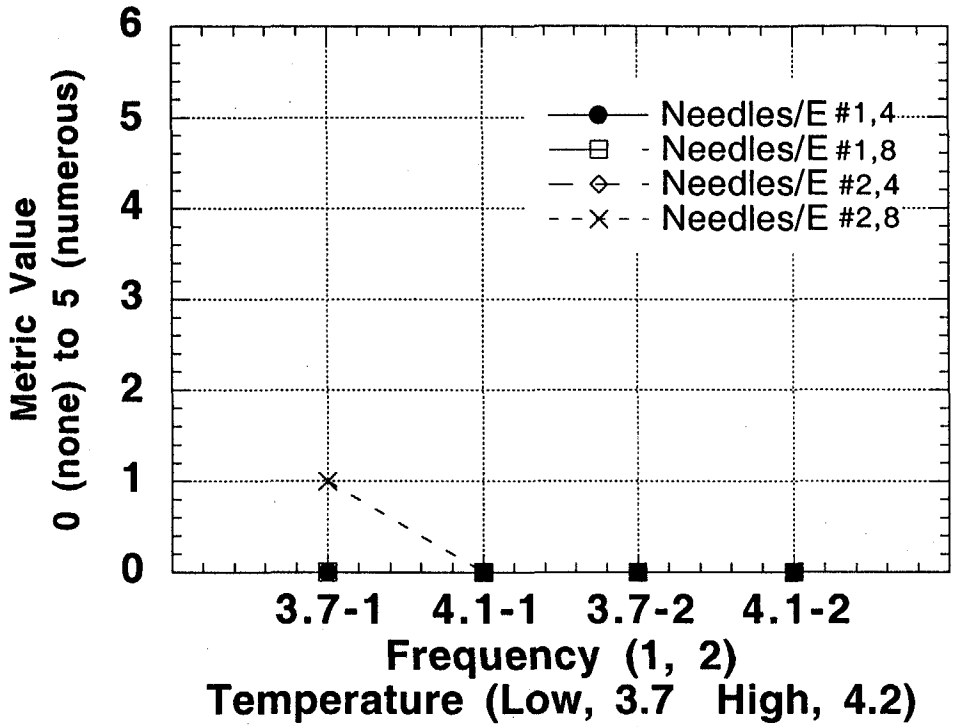
Metric Value
0 (none) to 5 (numerous)
6
5
4
3
2
1
0
Needles/E #1,4
Needles/E #1,8
Needles/E #2,4
Needles/E #2,8
3.7-1
4.1-1
3.7-2
4.1-2
Frequency (1, 2)
Temperature (Low, 3.7 High, 4.2)

Fig. 5(b)

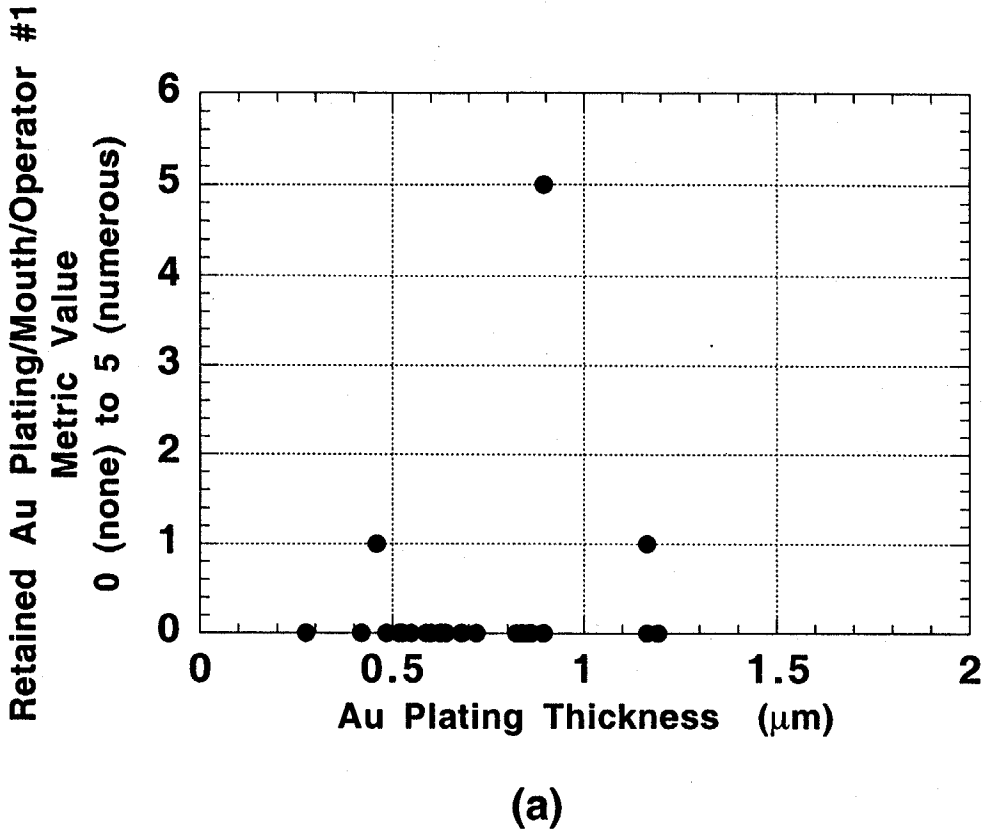


Fig. 6 Graphs of the retained Au layer metric at the "M" location for as a function of the recorded Au thickness: (a) operator #1 and (b) operator #2 . The presence of Au-Sn needles as a function of the starting Au thickness at locations "M," "C," and "E" is exemplified by the plots in (c), (d), and (e), respectively, for solder joints from the work of operator #2.

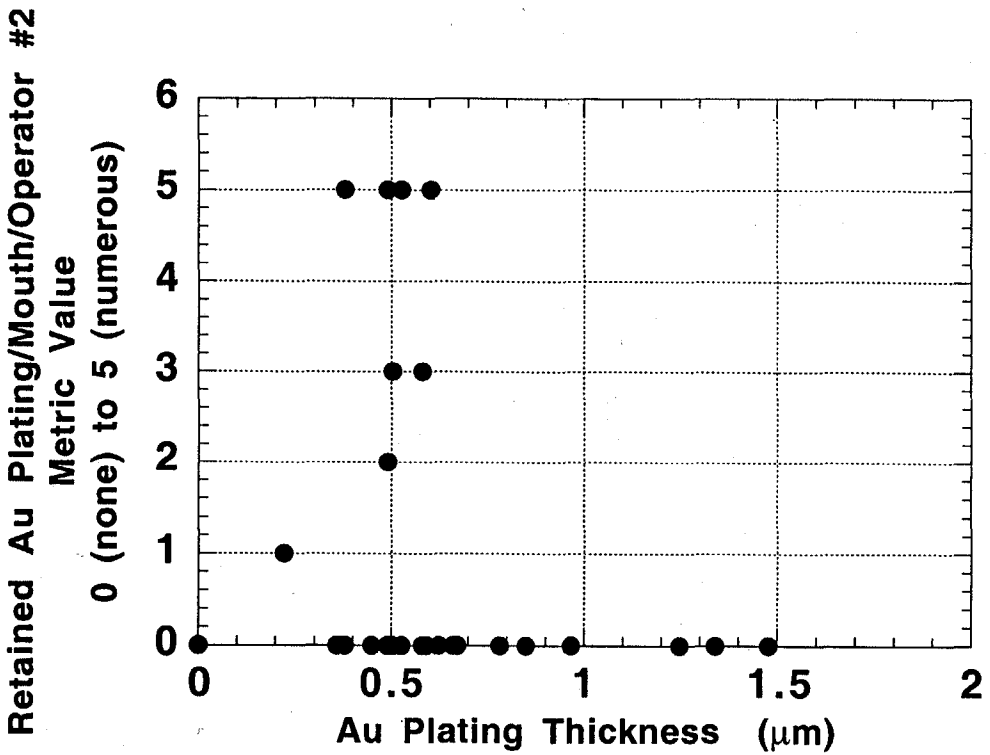
Retained Au Plating/Mouth/Operator #2
Metric Value
0 (none) to 5 (numerous)
6
5
4
3
2
1
0
0
0.5
1
1.5
2
Au Plating Thickness (μm)

Fig. 6(b)

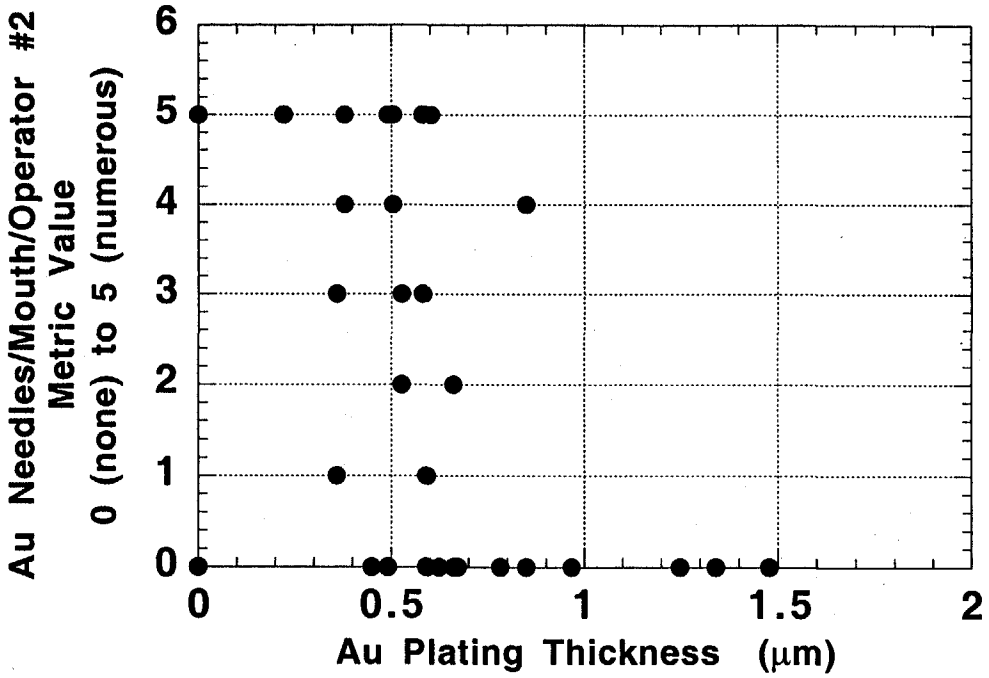
Au Needles/Mouth/Operator #2
Metric Value
0 (none) to 5 (numerous)
6
5
4
3
2
1
0
0
0.5
1
1.5
2
Au Plating Thickness (μm)

Fig. 6(c)

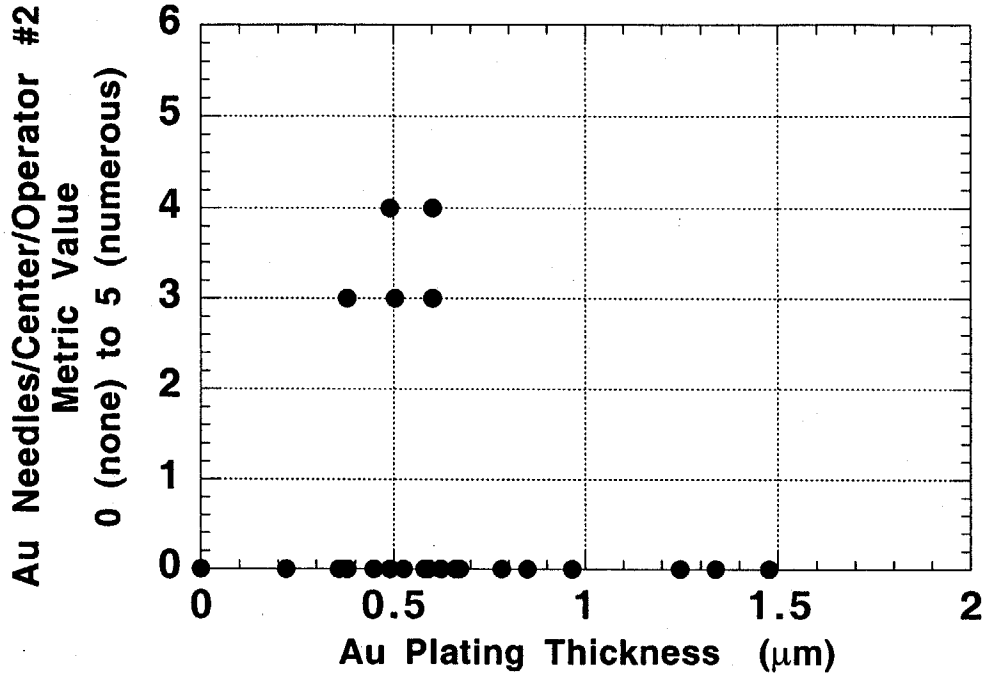
Au Needles/Center/Operator #2
Metric Value
0 (none) to 5 (numerous)
6
5
4
3
2
1
0
0
0.5
1
1.5
2
Au Plating Thickness (μm)

Fig. 6(d)

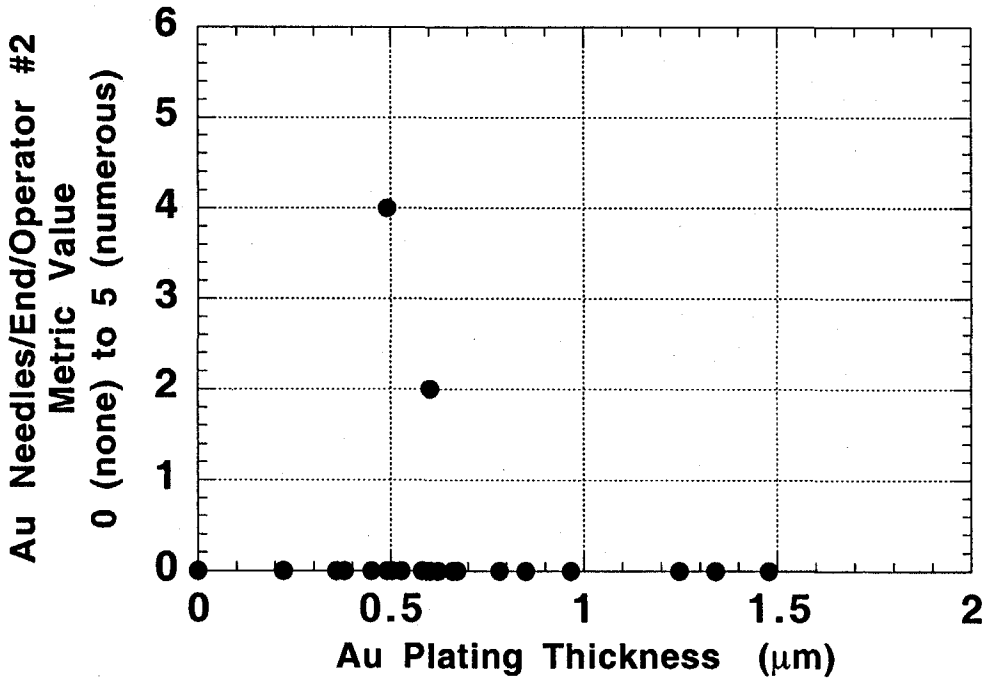
Au Needles/End/Operator #2
Metric Value
0 (none) to 5 (numerous)
6
5
4
3
2
1
0
0
0.5
1
1.5
2
Au Plating Thickness (μm)

Fig. 6(e)

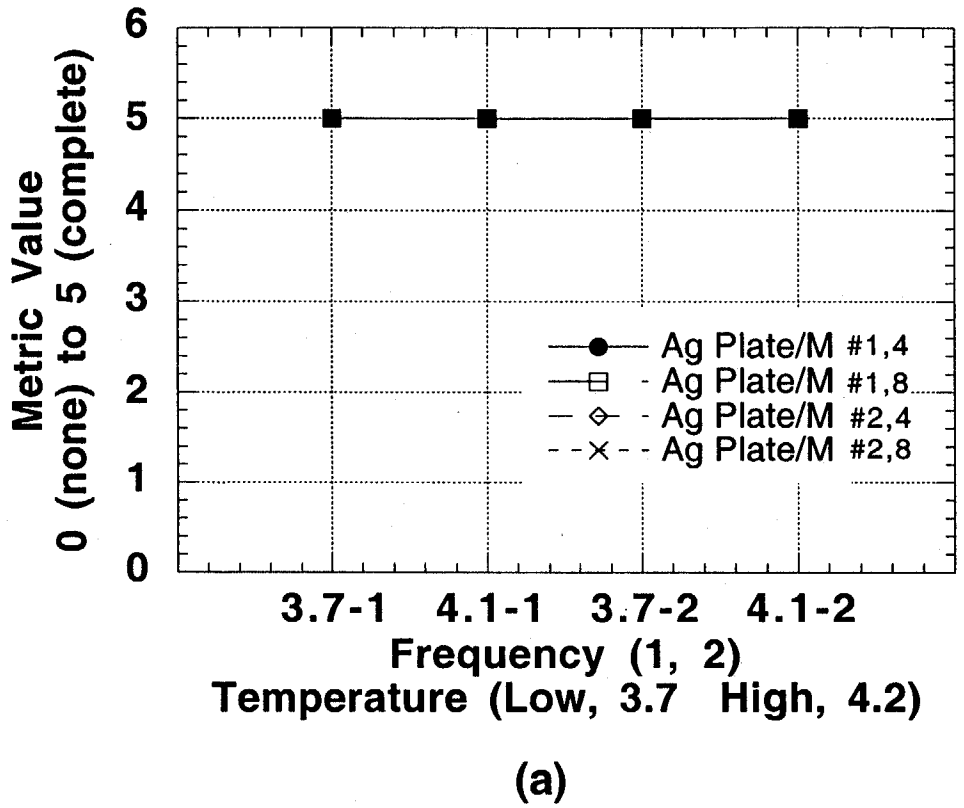


Fig. 7 (a) Graph of the retained Ag plating as a function of the soldering temperature (low, 3.7 and high, 4.1) and the wicking frequency (1 or 2) at the mouth location, "M," of the joint. (b) Graph of the retained Ag plating as a function of the soldering temperature (low, 3.7 and high, 4.1) and the wicking frequency (1 or 2) at the center location, "C," of the joint. (c) Graph of the retained Ag plating as a function of the soldering temperature (low, 3.7 and high, 4.1) and the wicking frequency (1 or 2) at the end location, "E," of the joint.

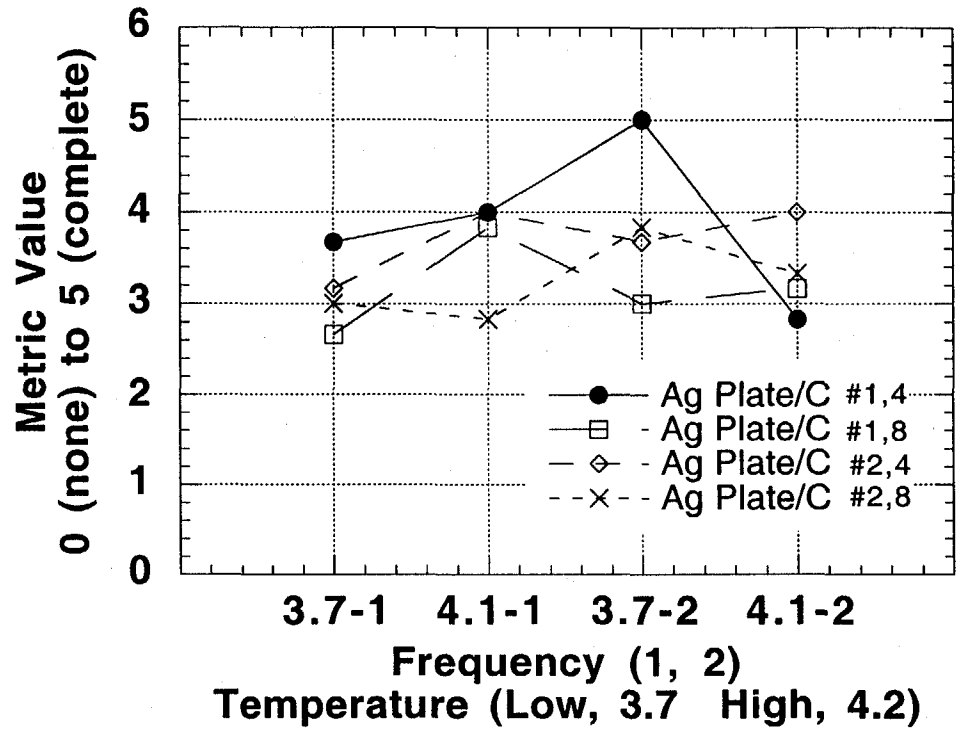
Metric Value
0 (none) to 5 (complete)
6
5
4
3
2
1
0
Ag Plate/C #1,4
Ag Plate/C #1,8
Ag Plate/C #2,4
Ag Plate/C #2,8
3.7-1
4.1-1
3.7-2
4.1-2
Frequency (1, 2)
Temperature (Low, 3.7 High, 4.2)

Fig. 7(b)

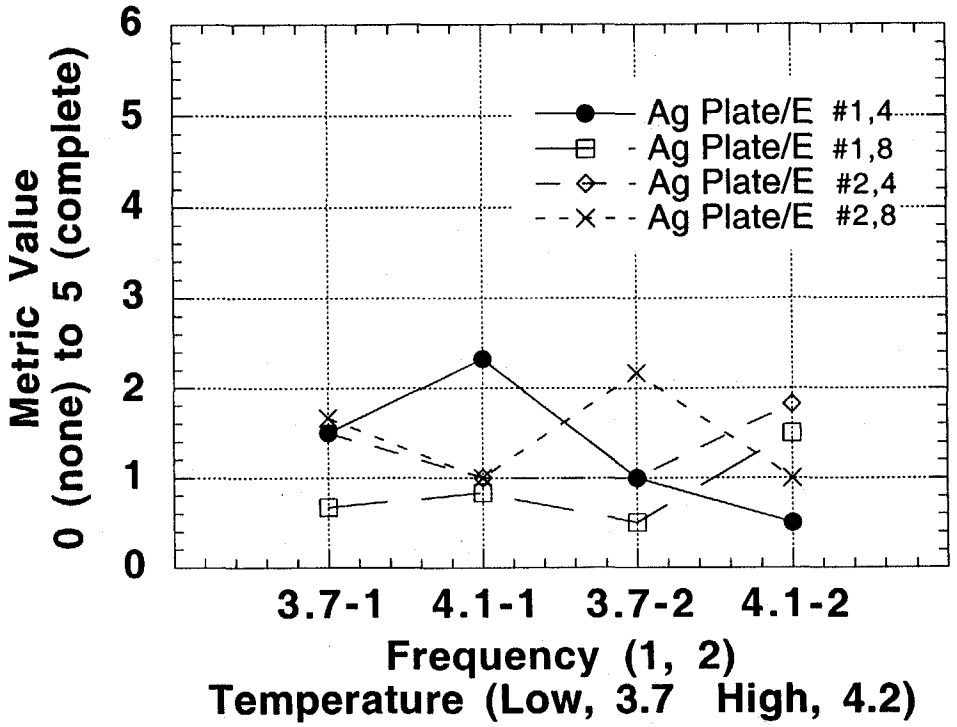
Metric Value
0 (none) to 5 (complete)
6
5
4
3
2
1
0
Ag Plate/E #1,4
Ag Plate/E #1,8
Ag Plate/E #2,4
Ag Plate/E #2,8
3.7-1
4.1-1
3.7-2
4.1-2
Frequency (1, 2)
Temperature (Low, 3.7 High, 4.2)

Fig. 7(c)